ACS APPLIED MATERIALS & INTERFACES

Research Article

www.acsami.org

Inhibitation of Cellular Toxicity of Gold Nanoparticles by Surface Encapsulation of Silica Shell for Hepatocarcinoma Cell Application

Qinghui Zeng,[†] Youlin Zhang,[†] Wenyu Ji,*[,†] Weiguang Ye,[†] Yinglei Jiang,[‡] and Jie Song*[,§]

[†]State Key Laboratory of Luminescence and Applications, Changchun Institute of Optics, Fine Mechanics and Physics, Chinese Academy of Sciences, Dong_Nanhu Road 3888, Changchun, Jilin 130033, P. R. China

[‡]Clinical Laboratory, the Affiliated Hospital to Changchun University of Chinese Medicine, Changchun, Jilin 130021, P. R. China

[§]Interdisciplinary Nanoscience Center (iNANO), Aarhus University, DK-8000 Aarhus C, Denmark

Supporting Information

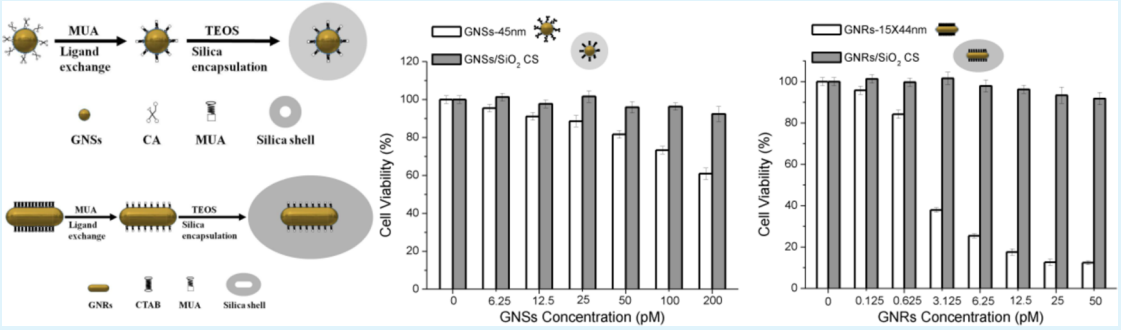

ABSTRACT: Nanotechnology, as a double-edged sword, endows gold nanoparticles (GNPs) more "power" in bioimaging and theragnostics, whereas an outstanding issue associated with the biocompatibility of GNPs should also be addressed. Especially for the silica-coated gold nanospheres (GNSs) and gold nanorods (GNRs), there is increasing attention to explore the application, because the surface silica encapsulation has been proved to be an alternative strategy for other organic surface coatings. However, among those reports there are very limited publications to focus on the toxicity of silica-coated GNSs and GNRs. Besides, the existing detoxification methods via surface chemistry on GNPs greatly improve the biocompatibility but still undergo challenges for high dose (>100 pM) demand and long-term stability. Here, we demonstrated a straightforward, low-cost, universal strategy for the surface chemistry on GNPs via silica encapsulating. Different size, shape, dose, and surface capping of GNPs for the nanotoxicity test have been carefully discussed. After silica encapsulating, the detoxification for all GNPs presents significantly from HepG2 cell proliferation results, especially for the GNRs. This new straightforward strategy will definitely rationalize the biocompatibility issue of GNPs and also provide potential for other surface chemistry methodology in biomedical fields.

KEYWORDS: *nanotoxicity, gold nanospheres, gold nanorods, HepG2 cells, cancer therapy, silica encapsulation*

1. INTRODUCTION

Recent advances in the synthesis of a variety of nanomaterials have shown a surge of interest due to numerous biomedical applications in the past decade, e.g., cellular imaging, biosensors, immunoassays, cancer diagnostic, therapy, etc.[1−6] Most of these applications are benefited from (1) surface functionalization for biocompatibility, molecular recognition, endocytosis efficiency, and so on and (2) their unique optical properties across the vis-NIR band.[3] Bulk gold along with gold-based compounds has been well-used in the clinic as well as other biomedicine applications, because of it being well-known for "safe" and chemically inert properties. Gold nanoparticles (GNPs), a key contribution from nanotechnology, now command a great deal of attention among those applications because of their chemically inert, favorable biocompatibility, controllability, variety, and versatility.[7,8] Despite the great excitement about the potential use of GNPs, researchers are increasingly aware that these in vivo bioapplications of the GNPs are severely restricted due to their health risks and cellular toxicity.[9] There are already tons of previous studies where the toxicity of GNPs has been investigated on various aspects, such as shape, size, surface chemistry, chemical composition, surface activity, and solubility.[8,10−14] Unfortunately, no simple conclusions have emerged from the above available reports, probably because of the variability of parameters such as the physical and chemical properties of the particles, cell type, dosing parameters, and the biochemical assays used.[15]

Although the toxicological mechanism of GNPs is still unclear, superior methodology has been employed to take precautions against the underlying nanotoxicity of GNPs. Chan et al. reported to tune the cellular uptake of GNPs by various

Received: August 12, 2014
Accepted: October 14, 2014
Published: October 14, 2014

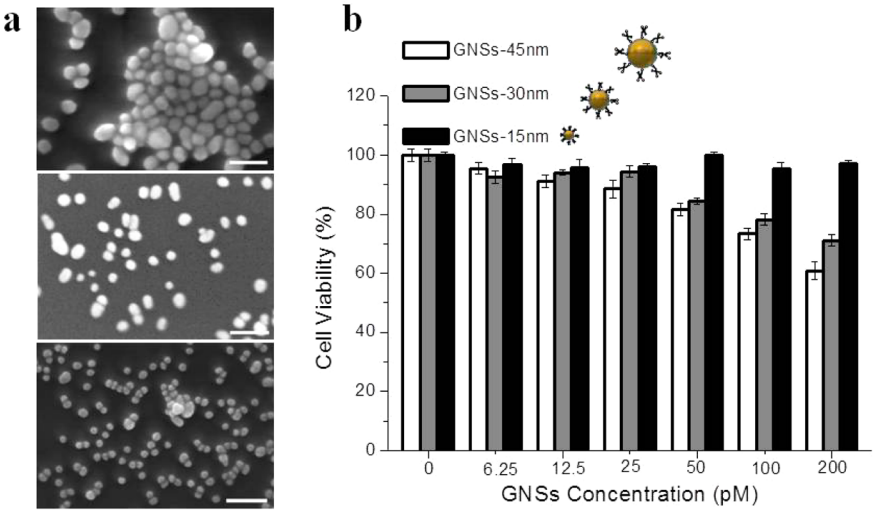

Figure 1. (a) FESEM images of differently sized GNSs and (b) effect of gold NPs on cell viability in HepG2 cells after 48 h treatment with the GNSs. The size of the GNSs is 45, 30, and 15 nm, respectively. The scale bar is 100 nm. The cell viability of control cells was set arbitrarily to 100%.

layer-by-layer polyelectrolyte (PE) coatings,[16] while Murphy and Wyatt et al. employed serum proteins, adsorb to GNPs, to eliminate the initial surface charge effect of the GNPs.[17] However, the organic modification by surface chemistry is still challenging to overcome the toxicity of GNPs under high dose (>100 pM). Inspired by Gao et al. work,[18] where the toxicity of quantum dots can be reduced by surface encapsulation of silica shell, the surface silica encapsulation should be an alternative strategy for other organic surface coating. In the nanotechnology field, the silica encapsulation on GNPs surface is an extremely mature method and can be traced back to the 1990s.[19] To our knowledge, the surface silica encapsulation has been proved to be an alternative strategy for other organic surface coating, and more evaluation on it will give more references for the further application of the silica-coated GNPs. However, to the best of our knowledge, the GNPs with surface silica encapsulation have not been investigated for the nanotoxicity, let alone systematic studies on different shapes, concentration, dose, and so on.

Besides, since hepatocarcinoma disease is the third leading cause of cancer-related deaths worldwide with >600,000 new incidents per year,[20,21] it calls for more and more attention to the research on hepatocarcinoma disease. From the view of cytology, HepG2 cells are generally used as a surrogate for human hepatocytes in pharmaceutical studies. Bartczak et al. have investigated the nanotoxicity of silica coated GNPs and shown that all the nanoparticles including the GNPs are founded noncytoxic in human endothelial cell lines.[22] However, it is worth to revaluate the nanotoxicity of silica coated GNPs on the HepG2 cell line because of the significant difference between the cancer cell and normal human endothelial cell.

In this work, we prepared the silica encapsulated gold nanospheres (GNSs) and gold nanorods (GNRs) and then investigated the inhibition of the nanotoxicity of these GNPs in human hepatocarcinoma cell line HepG2 cells. HepG2 cells were chosen for this study also because of the known difficulty of membrane translocation in the cell line as opposed to Hela cell lines.[14] To our knowledge, our research should be the first time to report the toxicity of silica-coated GNSs and GNRs for hepatocarcinoma disease. We observed that the nanotoxicity of all the gold NPs is dosage-dependent, but the nanotoxicity of the same shape NPs with a different size is different (15 nm GNSs vs 30 and 45 nm GNSs), the nanotoxicity of the same shape with a different surface group is different (e.g., citrate capped GNSs vs CTAB capped GNSs), and the nanotoxicity of the same-material metal nanoparticles with a different shape is different (e.g., GNSs vs GNRs). However, after the silica encapsulation the cellular toxicities of all the gold NPs mentioned above are restrained obviously. This work has systematically investigated the nanotoxicity of GNPs owning powerful plasmon absorption properties and has the potential to provide a uniform and systematic information estimation or reference when these GNPs are applied as probes in biological and medical fields. We also feel confident that our results will contribute to the exploring therapeutic method of hepatocarcinoma disease in the future.

2. EXPERIMENTAL SECTION

2.1. Chemicals. Fetal bovine serum (FBS), DMEM high glucose medium, penicillin, and streptomycin were obtained from Beyotime Institute of Biotechnology (Haimen, China). Sulforhodamine B (SRB), trichloroacetic acid (TCA), chloroauric acid trihydrate ($HAuCl_4 \cdot 3H_2O$, ≥99.9%), sodium borohydride ($NaBH_4$, ≥98%), sodium citrate (≥99%), and 11-mercaptoundecanoic acid (MUA, 98%) were purchased from Sigma-Aldrich (St. Louis, MO). Hexadecyltrimethylammonium bromide (CTAB, ~99%) and tetraethyl orthosilicate (TEOS, 98%) were purchased from Sigma. Deionized water was purified through a Milli-Q water purification system, and the resistivity was 18.2 MΩ·cm.

2.2. Synthesis and Characterization of Gold NSs. GNSs were prepared according to the standard sodium citrate reduction method. Typically, 45 mL of deionized water and 5 mL of $HAuCl_4$ (2.5 mM) aqueous solutions were mixed in a three-neck flask and heated to 100 °C. Subsequently, 1% sodium citrate solution was quickly added into the flask. The color of the solution rapidly changed from tint yellow to black and red or deep purple. After 1 h, the GNSs were cooled to room temperature waiting for the next nanotoxicity measurement. The size could be tuned by changing the volume of the additional sodium citrate. As shown in the field-emission scanning electron microscope (FESEM) of Figure 1a, the size of as-prepared GNSs was about 45 nm, 30 nm, and 15 nm, respectively. The metal plasmon field absorption peaks were localized at 530 nm, 525 nm, and 520 nm, respectively (Figure S1, Supporting Information). According to the plasmon resonance absorption spectrum of the GNSs, the concentration of the NPs investigated in our work can be calculated (see details in the

Supporting Information). The blue-shift of the absorption reflects the size effect of the GNPs.

2.3. Synthesis and Characterization of GNRs. The synthesis of GNRs was a traditionally seed-mediated growth procedure,[23−25] in which Au salt was reduced initially with a strong reducing agent in water at room temperature. Simply, the Au seed particles were prepared by reduction of $HAuCl_4$ (0.25 mM) in CTAB solution with the reduced reagent-ice-cold sodium borohydride. Subsequent reduction of more metal salt with a weak reducing agent, in the presence of structure-directing additives, leads to the controlled formation of GNRs. Briefly, a 25 mL growth solution was prepared by reduction of 0.5 mM $HAuCl_4$ in a solution containing CTAB, 0.05 mM silver nitrate, and 176 μL of ascorbic acid. The color of the solution rapidly changed from golden to colorless after the introduction of ascorbic acid. 36 μL of the seed solution was then added into the growth solution, and the color of the solution slowly changed from colorless to deep purple. Ultimately, the bilayer CTAB-coated gold NRs were obtained after several hours of stirring. The size of the prepared NRs was mainly 15 nm in width and 44 nm in length with plasmon absorption peaks at 517 (transverse plasmon band) and 714 nm (longitudinal plasmon band) (Figure S1, Supporting Information). According to the plasmon resonance absorption spectrum of the GNRs, the concentration of the NPs investigated in our work can be calculated (see details in the Supporting Information). The longitudinal plasmon band of the GNRs can be tuned well through varying the volume of the additional gold seed solutions or through the self-assembly growth method.[23−25] The red and near-infrared longitudinal plasmon band of the GNRs endows their wide applications, especially in the biological fields.

2.4. Synthesis and Characterization of Silica NSs. The silica NSs with a low polydispersity were synthesized according to the classical Stober method.[26] Typically, the TEOS and ammonia were added to the alcohol systems. After being stirred at room temperature for about 48 h, the resulting silica NSs can be obtained by centrifugation (8000 rpm) and redispersed in deionized water. The size of the silica NSs can be tuned by varying the ratio between TEOS and H_2O molecules. Generally, increasing the content of H_2O molecule inclines to synthesize bigger size silica NSs. When the molar ratio of TEOS/H_2O is decreased from 1:15 to 1:20 and 1:50, the size of the obtained silica NSs is increased from about 50 to 100 and 200 nm. The molar concentration of the silica NSs was calculated based on the consideration of the density of silica as 2.2 g/cm^3.[27]

2.5. Synthesis and Characterization of Silica Encapsulated Gold NSs. To transfer the citric acid (CA) coated GNSs into ethanol, the solutions were centrifuged or sedimented and the supernatant was removed. The MUA dissolved in ethanol was directly added into the GNSs aqueous solution, and the ratio of ethanol to water was set as 1 to 4. After 12 h, the solution was centrifuged for 15 min at 8000 rpm once. As-prepared differently sized gold NSs solution (20 mL) was mixed with isopropyl alcohol (80 mL) in a 150 mL glass conical tube. Under vigorous stirring, ammonia (1.92 mL, 30 wt %) was added to the mixed solution, followed by the addition of TEOS in isopropyl alcohol (0.6 mL, 10 mM) four times within 6 h (at a time interval of 2 h). After stirring for 18 h, the reaction mixture was then centrifuged at 8000 rpm for 15 min, and the GNSs/SiO_2 core/shell NP precipitate was redispersed into ethanol for further washing. After three times of washing, GNSs/SiO_2 core/shell NPs were obtained and redispersed into deionized water or ethanol (5 mL) for characterization. As shown in Figure S2 (see the Supporting Information), after the silica encapsulation, the plasmon absorption peak of the GNSs shift to the red by about 2−3 nm, which results from local dielectric constant changes near the metal core, and this phenomenon was in agreement with a previous report.[28] Additionally, the spectral shift was not accompanied by broadening of the spectra, indicating a lack of the NP aggregation.[29] As shown in the FESEM of Figure S3 (see the Supporting Information), the differently sized GNSs can be homogeneously encapsulated by the silica shell, and the resulting GNSs/SiO_2 core/shell NPs are monodispersed. It can be seen clearly that there are no independent GNSs, which prove the fact that the silica encapsulation is homogeneous and complete. After silica shell encapsulation, the size of the 15, 30, and 45 nm GNSs is increased to about 60−80 nm.

2.6. Synthesis and Characterization of Silica Encapsulated GNRs. The solubility of the CTAB-stabilized gold NRs was much smaller than that of citrate-stabilized GNSs, and they started to aggregate when the ratio of ethanol to water was greater than 0.25. Due to the relatively strong binding of the surfactant to the CTAB-stabilized GNRs, compared to citrate-stabilized GNSs, the reaction of coupling MUA on the GNRs' surface was different from the approach for citrate-stabilized gold NPs. The MUA dissolved in ethanol was directly added into the GNRs aqueous solution, and the ratio of ethanol to water was set as 1 to 9. After 12 h, the solution was centrifuged for 15 min at 8000 rpm once. The next synthesis procedure of silica-coated GNRs is the same as that of GNSs. As shown in Figure S2 (Supporting Information), after the silica encapsulation, the longitudinal surface plasmon absorption peak of the GNRs shift to the red by 9 nm, which also results from local dielectric constant changes near the metal core.[28] Additionally, the spectral shift was not accompanied by broadening of the spectra, indicating a lack of the NP aggregation.[29] The GNRs can be homogeneously encapsulated by the silica shell, and the resulting GNRs/SiO_2 core/shell NPs are monodispersed. It can be seen clearly that there are no independent GNRs, which prove the fact that the silica encapsulation is homogeneous and complete. After silica shell encapsulation, the 15 × 44 nm nanorods are changed to about 80 nm ellipsoids.

2.7. Cell Culture and SRB Assay. Human hepatocellular carcinoma HepG2 cells were maintained in DMEM high glucose medium supplemented with 10% FBS, 100 units/mL penicillin, and 100 μg/mL streptomycin in an atmosphere of 95% air and 5% CO_2 at 37 °C. The SRB assay is routinely used for cytotoxicity determination, based on the measurement of live cell protein content. It was performed in 96-well plates in octuplicate after 48 h treatment. In brief, cells were seeded at a density of 5×10^3 cells/well overnight and treated with the indicated concentrations of NPs for 48 h. Afterward, 100 μL of 20% TCA was added to the culture medium in each well and refrigerated at 4 °C for 3 h, then the supernatant was discarded, and the plate was washed for 5 times with water and air-dried. 100 μL of SRB solution 0.4% (w/v) in 1% acetic acid was added to each well and incubated for 30 min at room temperature. Unbounded SRB was flicked off the plates and air-dried the plates. Bound SRB was solubilized with 150 μL of 10 mM Tris-HCl to each well, and the plate was shaken for 5 min. The optical density (OD) at 570 nm wavelength was measured, and the ratio of cell viability to control group was calculated from the SRB data. The concern that various nanaoparticles, such as GNSs and GNRs in 570 nm, would interfere with the SRB determination was resolved by rinsing off the excess NPs which resided outside the cell or adhered to the dead cells in SRB assay procedure.[30] The control group also goes through the same process for SRB assay except for the NPs treatment.

3. RESULTS AND DISCUSSION

3.1. Naontoxicity of Citrate Capped GNSs on Cell Viability of HepG2 Cells. With the rapid appearance of gold NPs in biological applications, human exposure to gold NPs is unavoidable. However, a serious lack of knowledge regarding the health and safety issues of these NPs is genuinely felt. A very important question in nanotoxicological research concerns the factors that determine the cytotoxicity of nanomaterials. Obviously, one of the factors is related to size and surface chemistry.[31] Therefore, it is essential to investigate how size and surface properties affect the cytoxicity as well as other facets of NP-cell interactions. In order to interpret the results of such studies, it is essential that the investigated NPs are well characterized and comparable, so that only the size (or surface groups) is different, while other factors like composition, surface groups (or size), charge, etc. remain constant.

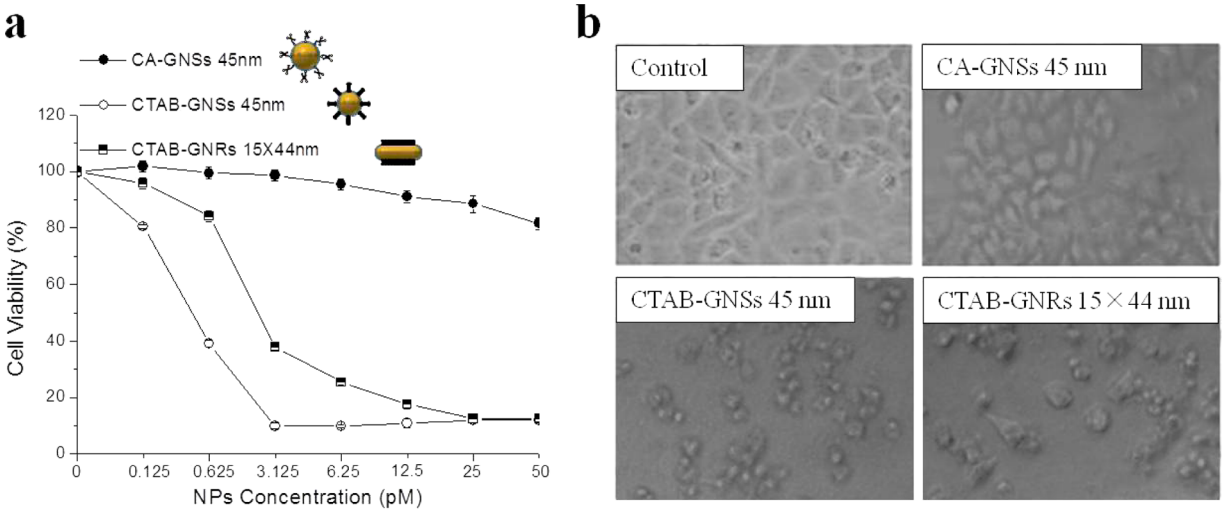

Figure 2. Effect of different surface groups and shape of gold NPs on cell viability and cell morphology in HepG2. (a) 45 nm CA and CTAB capped GNSs and CTAB-GNRs (15 × 44 nm) on cell viability. The cell viability of control cells was set arbitrarily to 100%. (b) HepG2 cell morphology in control, 45 nm CA-GNSs, 45 nm CTAB-GNSs and 15 × 44 nm CTAB-GNRs after 48 h treatment with the same concentration of 12.5 pM.

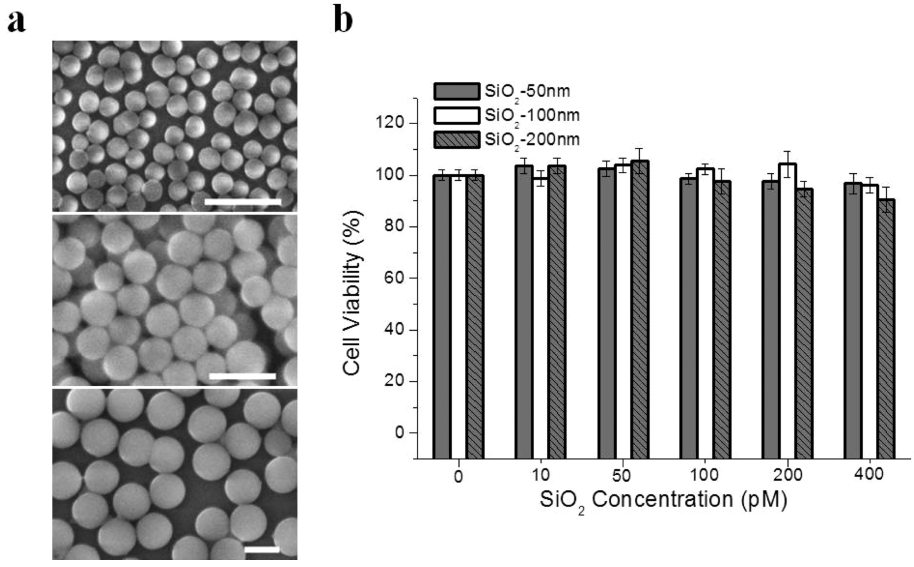

Figure 3. (a) FESEM images of 50, 100, and 200 nm silica NSs. The ratio of TEOS/H_2O is 1:15, 1:20, and 1:50 for the samples, respectively. The scale bar is 200 nm. (b) Effect of silica NSs on cell viability in HepG2 cells after 48 h treatment with 50, 100, and 200 nm silica NSs. The cell viability of control cells were set arbitrarily to 100%.

To determine if differently sized GNSs exhibit different cytotoxic effects on cancer cells, the HepG2 cells were exposed to different concentrations of GNSs for 48 h, and cell viability was measured to evaluate the cytotoxicity of the GNSs. As shown in Figure 1b, the cell viability of 15, 30, and 45 nm citrate sodium capped gold nanospheres in HepG2 cells was assessed after 48 h treatment with a series of concentrations of the NPs from 0 to 200 pM. It was shown that 15 nm GNSs did not influence cell growth even in the 200 pM concentration; however, 30 and 45 nm GNSs showed the reduction of HepG2 cells proliferation ratio by 28.9% and 39.1% in 200 pM compared with control group, respectively. The results indicated that the toxicity of GNSs was increased by the size-dependent manner.

3.2. Naontoxicity of CTAB Capped GNSs and GNRs on Cell Viability of HepG2 Cells. The influences of CTAB-capped GNSs on cell viability were measured in HepG2 cells with the same cultural conditions of the citrate-capped GNSs. It showed that significant damage was exhibited both in cell proliferation and cell morphology. As shown in Figure 2a, 0.625 pM CTAB-capped GNSs induced 60.9% reduction of cell survival rate in HepG2 cells, which showed the obviously higher nanotoxicity compared with the citrate capped GNSs (almost showed no nanotoxicity). The median inhibition concentration (IC50) of CTAB-GNSs in HepG2 cells is about 0.5 pM, which is significantly less than that of citrate-capped GNSs (more than 200 pM, see Figure 1b). It showed that significant damage was exhibited both in cell proliferation and cell morphology. This result indicated that the surface ligand played a key role on cell survival in this case. GNRs with the same surface group inhibited cell proliferation with the same trend to the 45 nm CTAB-capped GNSs. As shown in Figure 2a, 0.625 pM of GNRs induced 15.8% reduction of cell survival rate in HepG2 cells. The median inhibition concentration (IC50) of GNRs in

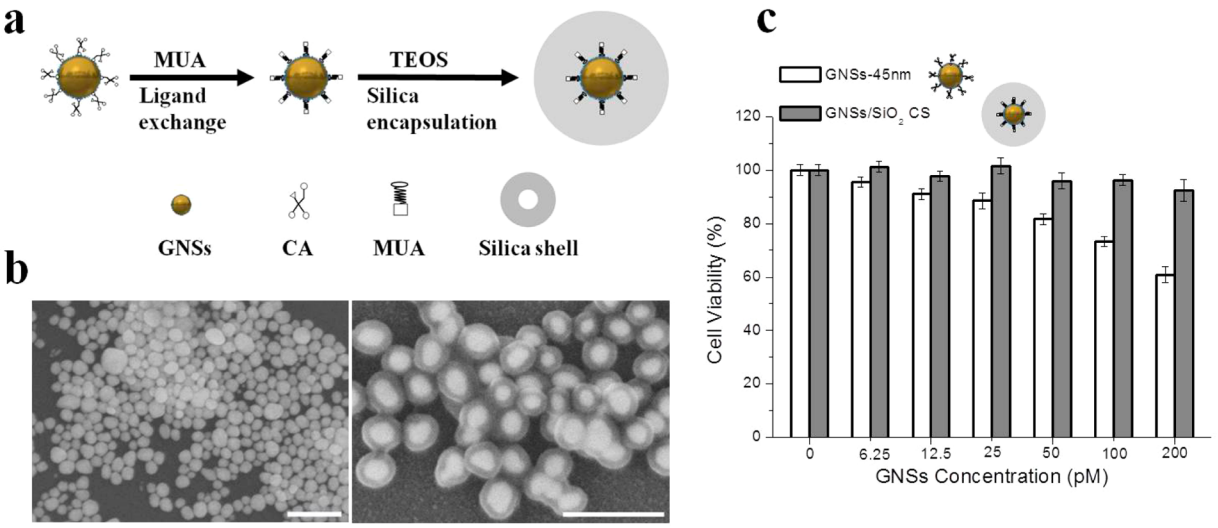

Figure 4. Effect of gold NPs on cell viability in HepG2 cells after 48 h treatment with the GNSs. (a) Schematic synthesis procedure of silica encapsulated GNSs. (b) FESEM results of 45 nm GNSs and GNSs/SiO_2 CS NPs, the scale bar is 200 nm. (c) Without and with silica shell encapsulation of 45 nm GNSs on cell viability in HepG2 cells. The cell viability of control cells were set arbitrarily to 100%.

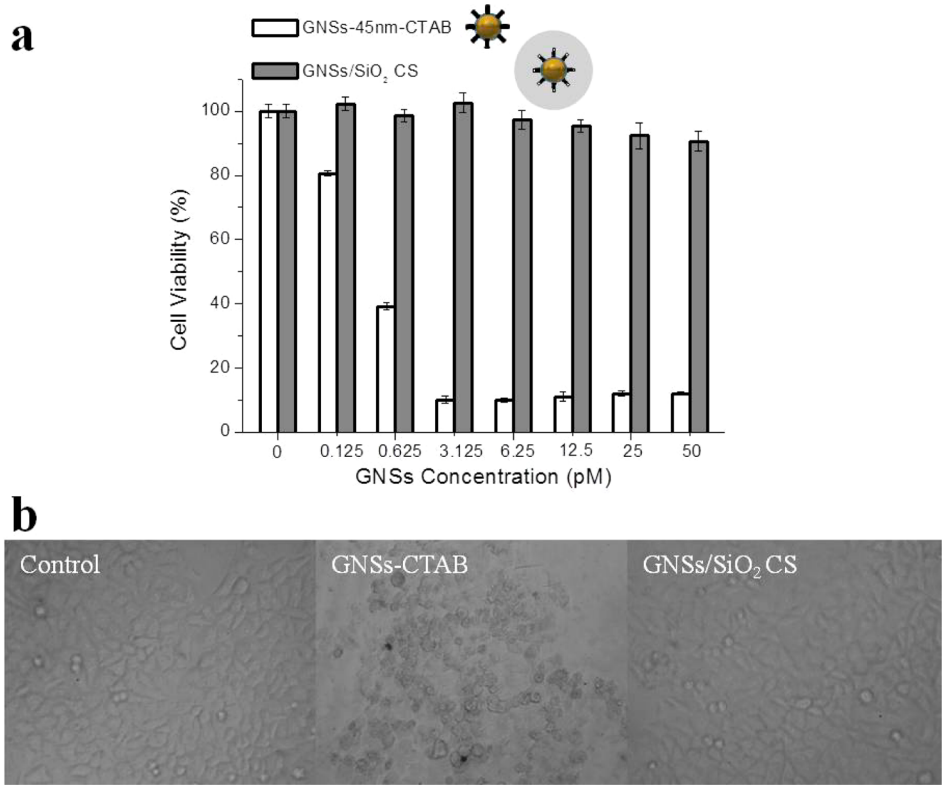

Figure 5. Effect of CTAB-capped GNSs on cell viability and cell morphology in HepG2 cells after 48 h treatment with the GNSs. (a) Without and with silica shell encapsulation of CTAB-capped GNSs on cell viability in HepG2 cells. The cell viability of control cells was set arbitrarily to 100%. (b) HepG2 cell morphology in control (left), 45 nm CTAB-GNSs (middle), and GNSs/SiO_2 CS (right) after 48 h treatment with the same concentration of 12.5 pM.

HepG2 cells is only 1.75 pM, which is significantly less than that of 45 nm citrate capped GNSs (more than 200 pM). When the concentration was higher than 0.125 pM, the CTAB-capped GNRs (15 × 44 nm) showed lower nanotoxicity compared to the CTAB-capped GNSs (45 nm), which was due to the larger surface area of the GNSs contacted with the HepG2 cells. We believe that based on the same dosage and surface properties, larger size NPs would cause a more toxic effect due to a larger function proportion of the NPs to the cell lines. It is reported that the surface charge plays a significant role in the process of cellular uptake.[31] This means that a larger particle size and a higher surface charge would often induce high nonspecific cellular uptake of NPs.[32] As a result, the larger size and a higher surface charge NPs will cause a relative obvious interaction with the cell line and lead to a serious cell toxicity. Shrunken cell membrane and cell debris were observed in HepG2 cells

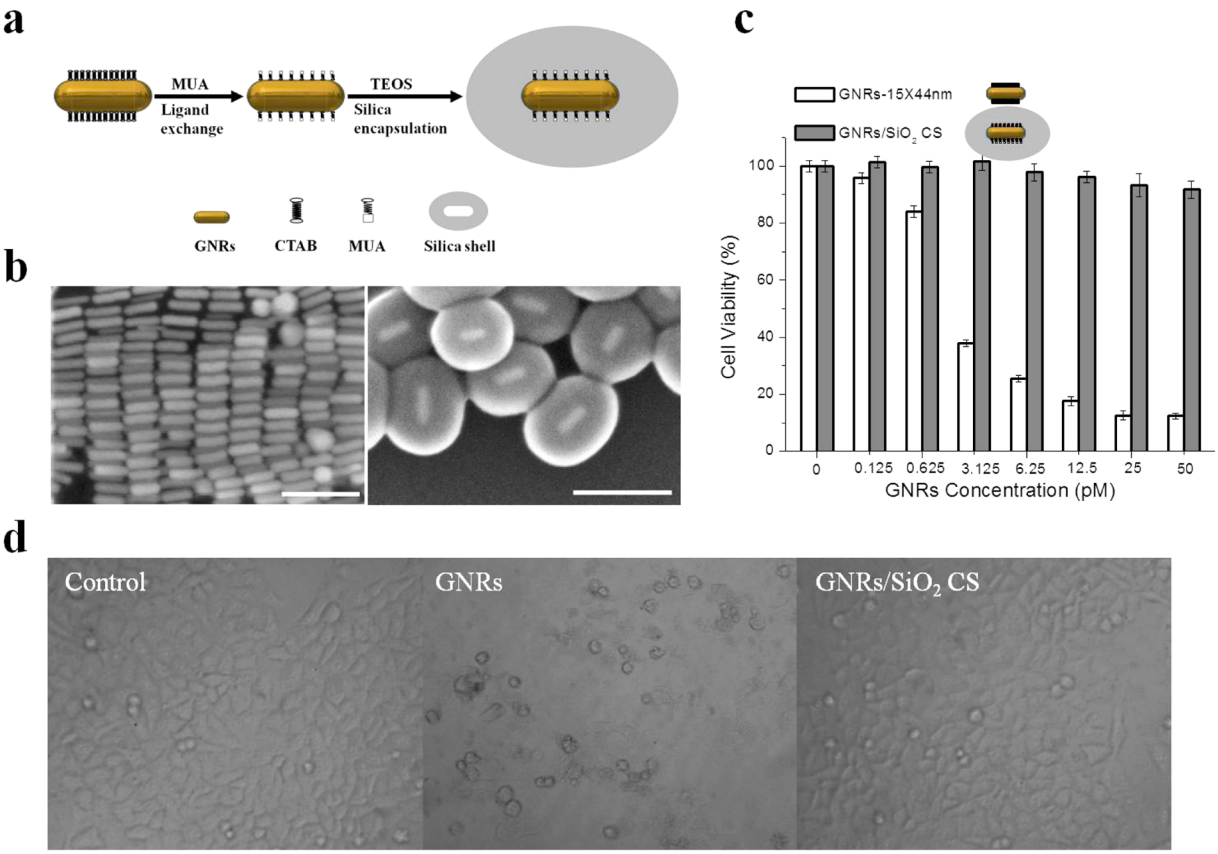

Figure 6. Without and with silica shell encapsulation of 15 × 44 nm GNRs on cell viability in HepG2 cells. (a) Schematic synthesis procedure of silica encapsulated GNRs. (b) FESEM results of 15 × 44 nm GNRs and GNRs/SiO_2 CS NPs, the scale bar is 100 nm. (c) Effect of gold NPs on cell viability in HepG2 cells after 48 h treatment with the GNRs. The cell viability of control cells were set arbitrarily to 100%. (d) Effect of gold NPs on cell morphology in HepG2 cells after 48 h treatment with the GNRs. HepG2 cell morphology in control (left), 15 × 44 nm CTAB-GNRs (middle), and GNRs/SiO_2 CS (right) after 48 h treatment with the same concentration of 12.5 pM.

treated with 12.5 pM CTAB capped GNSs and GNRs for 48 h (Figure 2b), which cellular morphologies were greatly different from the control sample.

3.3. Effect of Silica NSs on Cell Viability of HepG2 Cells. As shown in the FESEM of Figure 3a, when the molar ratio of TEOS/H_2O is decreased from 1:15 to 1:20 and 1:50, the size of the obtained silica NSs is increased from about 50 to 100 and 200 nm. As shown in Figure 3b, when the silica NSs were interacted with the HepG2 cells, the nanotoxicity was almost the same as the control sample when the concentration of the 50, 100, and 200 nm silica NSs was lower than 200 pmol/L. When the concentration of the three samples was as high as 400 pmol/L, only the 200 nm silica NSs showed the reduction of HepG2 cells proliferation ratio by 9.5%, while the relative smaller size (50 and 100 nm) silica NSs showed no toxicity at this concentration. This phenomenon proved two points: first, the silica NSs were safe to HepG2 cells for all sizes (50, 100, and 200 nm) when the concentration was lower than 200 pmol/L; second, the toxicity was size and concentration dependent, which follows the positive direction as size and concentration increased. The results further indicated that the toxicity of NPs was increased by the size-dependent manner.

3.4. Effect of Silica Shell Encapsulation to the Citrate Capped GNSs on Cell Viability of HepG2 Cells. Since the toxicity of GNSs was increased by the size-dependent manner, we selected the biggest size GNSs (45 nm) as a model to investigate the inhibition effect of cellular toxicity caused by the silica surface shell encapsulation. According to the new silica encapsulation method (see schematic synthesis procedure in Figure 4a), the GNSs can be homogeneously encapsulated by the silica shell, and the resulting GNSs/SiO_2 core/shell NPs are monodispersed. It can be seen clearly that there are no independent GNSs, which prove the fact that the silica encapsulation is homogeneous and complete (see the FESEM in Figure 4b). As shown in Figure 4c, after the silica encapsulation, the toxicity of the 45 nm GNSs was greatly inhibited, and the cell viability could be kept as high as 92.4% when the concentration of the GNS reached 200 pmol/L. This result sufficiently demonstrated the inhibition effect of cellular toxicity by the silica shell.

3.5. Effect of Silica Shell Encapsulation to the CTAB Capped GNSs on Cell Viability of HepG2 Cells. Since the silica encapsulation can inhibit the nanotoxicity of citrate capped GNSs, whether the fact that it will function on the more toxic CTAB capped GNSs seems more important to support our viewpoint. As shown in Figure 5a, after the silica encapsulation, the toxicity of the CTAB-capped GNSs was greatly inhibited, and the cell viability could be kept >90% when the concentration of the GNSs was lower than 50 pM. Shrunken cell membrane and cell debris were observed in HepG2 cells treated with 12.5 pM CTAB capped GNSs for 48 h (Figure 5b), which cellular morphology was greatly different from the control sample or the GNSs/SiO_2 CS NPs. This result sufficiently demonstrated the inhibition effect of cellular toxicity by the silica shell again.

3.6. Effect of Silica Shell Encapsulation to the CTAB Capped GNRs on Cell Viability of HepG2 Cells. To elucidate the cause of significant difference in cytotoxicity between differently shaped GNSs and GNRs, the impact of 15 × 44 nm CTAB capped GNRs was detected in HepG2 cells. Also according to the new silica encapsulation method (see schematic synthesis procedure in Figure 6a), the GNRs can be homogeneously encapsulated by the silica shell, and the resulting GNRs/SiO_2 core/shell NPs are monodispersed. It can be seen clearly that there are no independent GNRs, which prove the fact that the silica encapsulation is homogeneous and complete (see the FESEM in Figure 6b).

The nanotoxicity result is shown in Figure 6c, and it was not difficult to find that GNRs with the same surface group inhibited cell proliferation with the same trend to the 45 nm CTAB-capped GNSs (see Figure 2a) as the dose concentration was increased. It showed that a significant damage was exhibited both in cell proliferation and cell morphology. As shown in Figure 6c, 0.625 pM of GNRs induced 15.8% reduction of cell survival rate in HepG2 cells. The median inhibition concentration (IC50) of GNRs in HepG2 cells is only 1.75 pM, which is significantly less than that of 45 nm citrate capped GNSs (more than 200 pM). When the concentration was higher than 0.125 pM, the CTAB-capped GNRs (15 × 44 nm) showed lower nanotoxicity compared to the CTAB-capped GNSs (45 nm) (see Figure 2a), which was due to the larger surface area of the GNSs contacted with the HepG2 cells. We believe that based on the same dosage and surface properties, NPs with larger surface area would cause a more toxic effect due to a larger function proportion of the NPs to the cell lines. It is reported that the surface charge plays a significant role in the process of cellular uptake.[31] This means that a higher surface charge would often induce high nonspecific cellular uptake of NPs.[32] As a result, compared with the 15 × 44 nm GNRs, the 45 nm GNSs will cause a relative obvious interaction with the cell line and lead to a serious cell toxicity. However, similar to the result of the GNSs after the silica encapsulation, the toxicity of the GNRs was greatly inhibited, and the cell viability could be kept >90% when the concentration of the GNRs was lower than 50 pM. Shrunken cell membrane and cell debris were observed in HepG2 cells treated with 12.5 pM CTAB capped GNRs for 48 h (Figure 6d), which cellular morphology was greatly different from the control sample or the GNRs/SiO_2 CS NPs. This indicates that the nanotoxicity of the GNRs could also be inhibited via the surface silica shell encapsulation.

Cellular endocytosis, cellular delivery, and subcellular targeting inducing nanotoxicity of nanoparticles can be influenced in several ways.[32] The NPs have high surface-to-volume ratio, and thus a small change in the particle size, shape, and/or surface functional group may even lead to significant alteration in cellular interaction. Consequently, the cellular uptake, cytotoxicity, and subcellular localization of NPs are highly sensitive to the particle size, shape, surface charge, hydrophobicity, and nature of the surface ligands.[17] At the same time, NPs with a larger particle size and a higher surface charge would often induce high nonspecific cellular uptake but often end up at lysosomes and prevent subcellular targeting. This behavior further complicated the uptake activity of affinity ligands by reducing the specificity of NPs. Comparing with the influence of size or shape of the NPs, surface ligand seems to be a more crucial effect on the nanotoxicity of cells. For example, CTAB capped GNSs and GNRs were obviously more toxic than citrate sodium capped GNSs, because CTAB, as a well-known cationic surfactant, could increase cell membrane permeability and conjugate with nuclear acid;[33] and that is why Uboldi et al. and Freese et al. previously claimed that the size of the gold NPs was not a significant factor, but that the ligand on the particle surface was the cause for the increase of cytotoxicity.[34,35] For the focus topic on the toxicity of GNSs and GNRs, it can be seen that superior methodology has been employed mostly by surface chemistry, e.g. PE coating and OEG coating. Currently, the existing detoxification methods via surface chemistry on GNPs greatly improve the biocompatibility but still undergo challenges for high dose (>100 pM) demand and long-term stability. Besides, the traditional gold NPs with excellent biocompatibility have been widely applied in the biological and medical fields for a long time, while the silica NPs are always considered as the save materials based on the same dosage concentration. Instead of repeating the previous reports, we demonstrated a straightforward, low-cost, universal strategy for the surface chemistry on GNPs via silica encapsulating as well as different size, shape, dose, and surface capping of GNPs for the nanotoxicity test. Especially for the high dose nanotoxicity test, our reports will definitely rationalize the biocompatibility issue of GNPs and also provide potential for other surface chemistry methodology in biomedical fields.

On the other hand, more works are still absent to clarify the mechanism of silica coating NPs on cytotoxicity. Recently, a growing body of evidence indicated that the mechanism of NPs on cytotoxicity is mostly related with the induction of apoptosis in a living system. However, the initiators and signaling pathways of apoptosis are different, which is dependent on the special nature of NPs. Gao et al. reported gold NPs caused hydrogen oxygen accumulation by cytosolic glutathione depletion and subsequently activated mitochondrial apoptosis pathway.[36] Kang et al. stated that gold NPs localizing in cell nuclei would induce DNA damage and cytokinesis arrest.[37] Furthermore, the production of intracellular reactive oxygen species increased expression of cleaved caspase proteins and p53 activation were commonly involved in the mechanisms of apoptosis induced by NPs.[38−40] Therefore, it is also impossible to give simple conclusions from our results for the mechanisms of silica-coated GNSs and GNRs on HepG2, because of the variability of parameters such as the physical and chemical properties of the particles, dosing parameters, and the biochemical assays used.[15] To our knowledge, our research is the first time to report the toxicity of silica-coated GNSs and GNRs for hepatocarcinoma disease. It is hoped that the related results will contribute to the exploring therapeutic method of hepatocarcinoma disease in the future.

4. CONCLUSIONS

New biocompatible GNPs (including GNSs and GNRs) have been successfully fabricated via a straightforward, low-cost, universal strategy of surface chemistry --- silica encapsulating, which acts as an "agent" to reduce the nanotoxicity of these NPs in human hepatocarcinoma cell line HepG2 cells. The nanotoxicity of those GNPs without silica encapsulating is observed to be dependent on dosage, size, shape, and surface group. After the surface silica encapsulation, the cellular survival rate for all those GNPs can be improved from not more than 20% to over 90%, especially for the GNRs. This work has systematically investigated the nanotoxicity of GNPs owning powerful plasmon resonance absorption properties and has

provided a facile method to inhibit the cellular toxicity when they are applied. We hope this work has the potential to provide a uniform and systematic information estimation or reference when these NPs are applied as probes in biological and medical fields.

■ ASSOCIATED CONTENT

Supporting Information

The plasmon resonance absorption spectra of GNSs and GNRs (Figure S1), GNSs/SiO_2 and GNRs/SiO_2 core/shell NPs (Figure S2), and FESEM results of GNSs/SiO_2 core/shell NPs (Figure S3). This material is available free of charge via the Internet at http://pubs.acs.org.

■ AUTHOR INFORMATION

Corresponding Authors

*E-mail: song@inano.au.dk (J.S.).
*E-mail: jiwy@ciomp.ac.cn (W.Y.J.).

Notes

The authors declare no competing financial interest.

■ ACKNOWLEDGMENTS

This work was supported by the National Natural Science Foundation of China (61275197 and 61205025) and Science and Technology Development Project of Jilin Province under Grant No. 20130206105SF.

■ REFERENCES

(1) Qian, X. M.; Peng, X. H.; Ansari, D. O.; Yin-Goen, Q. Q.; Chen, G. Z.; Shin, D. M.; Yang, L. L.; Young, A. N.; Wang, M. D.; Nie, S. M. In Vivo Tumor Targeting and Spectroscopic Detection with Surface-enhanced Raman Nanoparticle Tags. *Nat. Biotechnol.* **2008**, *26*, 83−90.

(2) Zrazhevskiy, P.; Sena, M.; Gao, X. Designing Multifunctional Quantum Dots for Bioimaging, Detection, and Drug Delivery. *Chem. Soc. Rev.* **2010**, *39*, 4326−4354.

(3) Khlebtsov, N.; Dykman, L. Biodistribution and Toxicity of Engineered Gold Nanoparticles: A Review of In Vitro and In Vivo Studies. *Chem. Soc. Rev.* **2011**, *40*, 1647−1671.

(4) Law, W. C.; Yong, K. T.; Baev, A.; Prasad, P. N. Sensitivity Improved Surface Plasmon Resonance Biosensor for Cancer Biomarker Detection Based on Plasmonic Enhancement. *ACS Nano* **2011**, *5*, 4858−4864.

(5) Zhang, Z. J.; Wang, L. M.; Wang, J.; Jiang, X. M.; Li, X. H.; Hu, Z. J.; Ji, Y. L.; Wu, X. C.; Chen, C. Y. Mesoporous Silica-coated Gold Nanorods as a Light-mediated Multifunctional Theranostic Platform for Cancer Treatment. *Adv. Mater.* **2012**, *24*, 1418−1423.

(6) Song, J.; Chen, M. L.; Regina, V. R.; Wang, C. X.; Meyer, R. L.; Xie, E. Q.; Wang, C.; Besenbacher, F.; Dong, M. D. Safe and Effective Ag Nanoparticles Immobilized Antimicrobial NanoNonwovens. *Adv. Eng. Mater.* **2012**, *14*, B240−B246.

(7) Boisselier, E.; Astruc, D. Gold Nanoparticles in Nanomedicine: Preparations, Imaging, Diagnostics, Therapies and Toxicity. *Chem. Soc. Rev.* **2009**, *38*, 1759−1782.

(8) Murphy, C. J.; Gole, A. M.; Stone, J. W.; Sisco, P. N.; Alkilany, A. M.; Goldsmith, E. C.; Baxter, S. C. Gold Nanoparticles in Biology: Beyond Toxicity to Cellular Imaging. *Acc. Chem. Res.* **2008**, *41*, 1721−1730.

(9) Kong, B.; Seog, J. H.; Graham, L. M.; Lee, S. B. Experimental Considerations on the Cytotoxicity of Nanoparticles. *Nanomedicine* **2011**, *6*, 929−941.

(10) Connor, E. E.; Mwamuka, J.; Gole, A.; Murphy, C. J.; Wyatt, M. D. Gold Nanoparticles Are Taken up by Human Cells But Do Not Cause Acute Cytotoxicity. *Small* **2005**, *1*, 325−327.

(11) Oberdörster, G.; Stone, V.; Donaldson, K. Toxicology of Nanoparticles: A Historical Perspective. *Nanotoxicology* **2007**, *1*, 2−25.

(12) Chithrani, B. D.; Ghazani, A. A.; Chan, W. C. W. Determining the Size and Shape Dependence of Gold Nanoparticle Uptake into Mammalian Cells. *Nano Lett.* **2006**, *6*, 662−668.

(13) Thomas, M.; Klibanov, A. M. Conjugation to Gold Nanoparticles Enhances Polyethylenimine's Transfer of Plasmid DNA into Mammalian Cells. *Proc. Natl. Acad. Sci. U. S. A.* **2003**, *100*, 9138−9143.

(14) Tkachenko, A. G.; Xie, H.; Coleman, D.; Glomm, W.; Ryan, J.; Anderson, M. F.; Franzen, S.; Feldheim, D. L. Multifunctional Gold Nanoparticle−Peptide Complexes for Nuclear Targeting. *J. Am. Chem. Soc.* **2003**, *125*, 4700−4701.

(15) Alkilany, A.; Murphy, C. Toxicity and Cellular Uptake of Gold Nanoparticles: What We Have Learned So Far? *J. Nanopart. Res.* **2010**, *12*, 2313−2333.

(16) Hauck, T. S.; Ghazani, A. A.; Chan, W. C. W. Assessing the Effect of Surface Chemistry on Gold Nanorod Uptake, Toxicity, and Gene Expression in Mammalian Cells. *Small* **2008**, *4*, 153−159.

(17) Alkilany, A. M.; Nagaria, P. K.; Hexel, C. R.; Shaw, T. J.; Murphy, C. J.; Wyatt, M. D. Cellular Uptake and Cytotoxicity of Gold Nanorods: Molecular Origin of Cytotoxicity and Surface Effects. *Small* **2009**, *5*, 701−708.

(18) Hu, X. G.; Gao, X. H. Silica-polymer Dual Layer-encapsulated Quantum Dots with Remarkable Stability. *ACS Nano* **2010**, *4*, 6080−6086.

(19) Dick, K.; Dhanasekaran, T.; Zhang, Z.; Meisel, D. Size-dependent Melting of Silica-encapsulated Gold Nanoparticles. *J. Am. Chem. Soc.* **2002**, *124*, 2312−2317.

(20) Hynes, R. O. Integrins: Bidirectional, Allosteric Signaling Machines. *Cell* **2002**, *110*, 673−687.

(21) Brakebusch, C.; Fassler, R. Beta 1 Integrin Function In Vivo: Adhesion, Migration and More. *Cancer Metastasis Rev.* **2005**, *24*, 403−411.

(22) Bartczak, D.; Muskens, O. L.; Nitti, S.; Sanchez-Elsner, T.; Millar, T. M.; Kanaras, A. G. Interactions of Human Endothelial Cells with Gold Nanoparticles of Different Morphologies. *Small* **2012**, *8*, 122−130.

(23) Nikoobakht, B.; El-Sayed, M. A. Preparation and Growth Mechanism of Gold Nanorods (NRs) Using Seed-mediated Growth Method. *Chem. Mater.* **2003**, *15*, 1957−1962.

(24) Orendorff, C. J.; Murphy, C. J. Quantitation of Metal Content in the Silver-assisted Growth of Gold Nanorods. *J. Phys. Chem. B* **2006**, *110*, 3990−3994.

(25) Zeng, Q. H.; Zhang, Y. L.; Liu, X. M.; Tu, L. P.; Kong, X. G.; Zhang, H. Multiple Homogeneous Immunoassays Based on A Quantum dots−Gold Nanorods FRET Nanoplatform. *Chem. Commun.* **2012**, *48*, 1781−1783.

(26) Stober, W.; Fink, A.; Bohn, E. Controlled Growth of Monodisperse Silica Spheres in Micron Size Range. *J. Colloid Interface Sci.* **1968**, *26*, 62.

(27) Yu, T.; Malugin, A.; Ghandehari, H. Impact of Silica Nanoparticle Design on Cellular Toxicity and Hemolytic activity. *ACS Nano* **2011**, *5*, 5717−5728.

(28) Kelly, K. L.; Coronado, E.; Zhao, L. L.; Schatz, G. C. The Optical Properties of Metal Nanoparticles: The Influence of Size, Shape, and Dielectric Environment. *J. Phys. Chem. B* **2003**, *107*, 668−677.

(29) Aslan, K.; Perez-Luna, V. H. Surface Modification of Colloidal Gold by Chemisorption of Alkanethiols in The Presence of A Nonionic Surfactant. *Langmuir* **2002**, *18*, 6059−6065.

(30) Vichai, V.; Kirtikara, K. SRB Colorimetric Assay for Cytotoxicity Screening. *Nat. Protoc.* **2006**, *1*, 1112−1116.

(31) Bhattacharjee, S.; Ershov, D.; Fytianos, K.; Gucht, J.; Alink, G. M.; Rietjens, I. M. C. M.; Marcelis, A. T. M.; Zuilhof, H. Cytotoxicity and Cellular Uptake of Tri-block Copolymer Nanoparticels with Different Size and Surface Characteristics. *Part. Fibre Toxicol.* **2012**, *9*, 11.

(32) Tan, S. J.; Jana, N. R.; Gao, S. J.; Patra, P. K.; Ying, J. Y. Surface-ligand-dependent Cellular Interaction, Subcellular Localization, and Cytotoxicity of Polymer-coated Quantum Dots. *Chem. Mater.* **2010**, *22*, 2239−2247.

(33) Qiu, Y.; Liu, Y.; Wang, L. M.; Xu, L. G.; Bai, R.; Ji, Y. L.; Wu, X. C.; Zhao, Y. L.; Li, Y. F.; Chen, C. Y. Surface Chemistry and Aspect Ratio Mediated Cellular Uptake of Au Nanorods. *Biomaterials* **2010**, *31*, 7606−7619.
(34) Uboldi, C.; Bonacchi, D.; Lorenzi, G.; Hermanns, M. I.; Pohl, C.; Baldi, G.; Unger, R. E.; Kirkpatrick, C. J. Gold Nanoparticles Induce Cytotoxicity in The Alveolar Type-II Cell Lines A549 and NCIH441. *Part. Fibre Toxicol.* **2009**, *6*, 18−29.
(35) Freese, C.; Uboldi, C.; Gibson, M. I.; Unger, R. E.; Weksler, B. B.; Romero, I. A.; Couraud, P. O.; Kirkpatrick, C. J. Uptake and Cytotoxicity of Citrate-coated Gold Nanospheres: Comparative Studies on Human Endothelia and Epithelial Cells. *Part. Fibre Toxicol.* **2012**, *9*, 23−33.
(36) Gao, W.; Xu, K.; Ji, L.; Tang, B. Effect of Gold Nanoparticles on Glutathione Depletion-induced Hydrogen Peroxide Generation and Apoptosis in HL7702 Cells. *Toxicol. Lett.* **2011**, *205*, 86−95.
(37) Kang, B.; Mackey, M. A.; El-Sayed, M. A. Nuclear Targeting of Gold Nanoparticles in Cancer Cells Induces DNA Damage, Causing Cytokinesis Arrest and Apoptosis. *J. Am. Chem. Soc.* **2010**, *132*, 1517−1519.
(38) Eom, H. J.; Choi, J. p38 MAPK Activation, DNA Damage, Cell Cycle Arrest and Apoptosis as Mechanisms of Toxicity of Silver Nanoparticles in Jurkat T Cells. *Environ. Sci. Technol.* **2010**, *44*, 8337−8342.
(39) Gopinath, P.; Gogoi, S. K.; Sanpui, P.; Paul, A.; Chattopadhyay, A.; Ghosh, S. S. Signaling Gene Cascade in Silver Nanoparticle Induced Apoptosis. *Colloids Surf., B* **2010**, *77*, 240−245.
(40) Wu, J.; Sun, J.; Xue, Y. Involvement of JNK and P53 Activation in G2/M Cell Cycle Arrest and Apoptosis Induced by Titanium Dioxide Nanoparticles in Neuron Cells. *Toxicol. Lett.* **2010**, *199*, 269−276.